

Journal of Materials Chemistry A

Accepted Manuscript



This is an *Accepted Manuscript*, which has been through the Royal Society of Chemistry peer review process and has been accepted for publication.

Accepted Manuscripts are published online shortly after acceptance, before technical editing, formatting and proof reading. Using this free service, authors can make their results available to the community, in citable form, before we publish the edited article. We will replace this *Accepted Manuscript* with the edited and formatted *Advance Article* as soon as it is available.

You can find more information about *Accepted Manuscripts* in the [Information for Authors](#).

Please note that technical editing may introduce minor changes to the text and/or graphics, which may alter content. The journal's standard [Terms & Conditions](#) and the [Ethical guidelines](#) still apply. In no event shall the Royal Society of Chemistry be held responsible for any errors or omissions in this *Accepted Manuscript* or any consequences arising from the use of any information it contains.

Cite this: DOI: 10.1039/c0xx00000x

www.rsc.org/xxxxxx

ARTICLE TYPE

Environmentally Friendly Biomaterials as an Interfacial Layer for Highly Efficient and Air-stable Inverted Organic Solar Cells

Riming Nie, ^a Aiyuan Li, ^a and Xianyu Deng^{*a}⁵ Received (in XXX, XXX) Xth XXXXXXXXXX 20XX, Accepted Xth XXXXXXXXXX 20XX

DOI: 10.1039/b000000x

An appropriate interfacial modification plays important roles on the high performance in organic solar cells. We report that the transparent cathode of indium tin oxide (ITO), by modification with ultrathin layer of environmentally friendly biomaterials of peptides, has an effective work function reduction. The device investigation exhibits that the power conversion efficiency (PCE) was significantly increased from 2.12% to 8.13% with the use of the peptide modification. The inverted device with peptide-modified ITO as cathode showed significantly longer time efficiency delay in air than conventional forward devices with an active metal as cathode. Because the peptides are biological materials naturally existed in lots of life bodies, the results provide an environmentally safe and healthy method to fabricate highly efficient and air-stable organic solar cells.

15 Introduction

Organic based solar cells (OSCs) have been attracting growing interests due to their unique advantages, such as low fabrication cost, light weight, and high mechanical flexibility, all of which enable them for potential applications in low-cost and renewable energy sources.¹⁻⁴ With the continuous improvement of organic solar cells, the future of fabrication will be required for more environmentally friendly and better integration of green technology for sustainable organic devices. In organic materials, biomaterials and natural compound have especial advantages that they are environmentally friendly, and can be naturally occurring so that they can sustainably contribute to organic electronics. However, despite these advantages, few biomaterials have been reported as functional elements in the fabrication of organic based solar cells. Here, we report the use of peptide, the widely existent biomaterial in biology, as an interfacial modifier in the fabrication of organic solar cells.

The basic structure of organic solar cells includes a bulk heterojunction layer, where conjugated polymers act as electron donors and fullerene derivatives act as electron acceptors, which are sandwiched by a bottom electrode of transparent indium tin oxide (ITO) and a metal counter electrode. Compared with the conventional forward organic solar cells, where the ITO is a hole collection electrode, inverted organic solar cells with the ITO as an electron collection electrode are more stable due to the lack of acidic conducting polymer and active metal.⁵⁻⁸ The inverted solar cells also take advantage of vertical phase separation, which results in acceptor materials that are richer near the bottom electrode and donor materials that are richer near the top electrode.⁹ However, ITO electrodes generally do not have good electron selectivity because their work-function (about 4.7 eV) is seriously mismatched with the lowest unoccupied molecular orbit (LUMO) energy level of organic acceptors. Therefore, lowering the work-function of the ITO is the key for

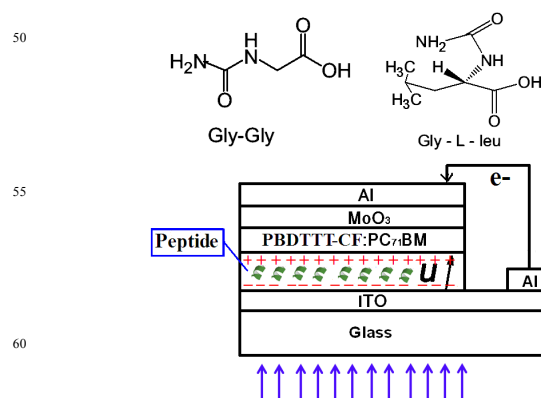


Fig.1. Molecular structures of the two peptides and device schematic of the inverted organic solar cells.

realizing highly efficient inverted organic solar cells. Some alternative methods were employed to overcome the problem of work-function mismatch. One method was the insertion of an n-type metal oxide between the ITO and the organic active layer, including TiO_x, ZnO_x, or an interfacial layer of alkali metal salts, such as Cs₂CO₃.¹⁰⁻¹³ Another method was solution-depositing a layer of 5-10 nm organic materials on top of the ITO, including polymer electrolytes, neutral insulative polymers and zwitterions.¹⁴⁻²⁰ These additional layers can adjust the energy barrier and form an electron selective contact between the ITO and the organic active layer, resulting in largely enhanced electron collection efficiency and an effective increased open-circuit voltage (Voc). However, the inserted layers have intrinsic drawbacks that they would unavoidably affect properties such as the conductivity, the transparency, and the surface roughness of the ITO. To overcome this shortcoming, modifying the ITO surface with a self-assembled molecular monolayer (SAM) was employed, since SAM requires only a small amount of materials

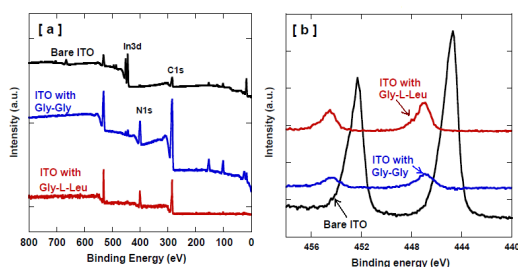


Fig. 2. Survey and high-resolution XPS profiles of In 3d acquired from the bare ITO, the ITO with Gly-Gly and the ITO with Gly-L-Leu.

and it can tune the surface work function with little changes on the bulk electrical properties. Several SAMs have been reported to lower the ITO work function. These SAM materials include $N(C_4H_9)_4OH$, tetrakis (dimethylamino) ethylene (TDAE), and 3-aminopropyltriethoxysilane (APTES).²¹⁻²³ However, most of the previous SAM materials are chemically toxic and processed in organic solvents, which are unhealthy and harmful to the environment.

In this contribution, we report the results of the modification of ITO with SAM of nontoxic and water soluble biomaterial of peptide. It significantly lowered the work function of the ITO and provided a good match of energy levels of the ITO and organic active materials to achieve highly efficient and air-stable inverted OSCs. **Fig. 1** shows the device structure, where the active layer is the blend of poly[4,8-bis(2-ethylhexyloxy)-benzo[1,2-b:4,5-b']dithiophene-2,6-diyl-alt-(4-octanoyl-5-fluoro-thieno[3,4-b]thiophene-2-carboxylate)-2,6-diyl] (PBDTTT-CF) and phenyl- C_{71} -butyric acid methyl ester (PC₇₁BM), and the chemical structure of two peptides of glycylglycine (Gly-Gly) and glycine-L-leucine (Gly-L-Leu) used in this study. Because the structure of the peptides contains carboxylic acid group (-COOH), the peptides can be chemically adsorbed on the surface of a metal oxide by the reaction of -COOH with metal oxide or -OH on the metal oxide surface. The peptide adsorbed on ITO surface produces molecule dipole moments arranged on the surface. Consequently, the work function of the ITO can be largely reduced to achieve the high-efficiency of the inverted organic solar cells. X-ray and ultraviolet photoelectron spectroscopy (XPS and UPS) were measured to investigate the work function of ITO substrates and the effect of peptides SAMs on surface composition.

Results and Discussion

Fig. 2(a) shows the full spectrum of XPS acquired from the bare ITO, Gly-Gly treated ITO, and Gly-L-Leu treated ITO after the water rinse. The appearance of the N1s peak related to the -N-proximal to 400 eV, and the disappearance or weakness of the peaks for indium atom orbits on the Gly-Gly deposited ITO clearly demonstrates the adsorption of Gly-Gly on the surface of ITO. From the high-resolution XPS picture as shown in **Fig. 2(b)**, an obvious shift occurred in the peak of the In3d on the Gly-Gly treated ITO compared to the bare ITO, which proved the chemical adsorbed monolayer of Gly-Gly on top of ITO. A similar phenomenon was also observed for the other peptide Gly-

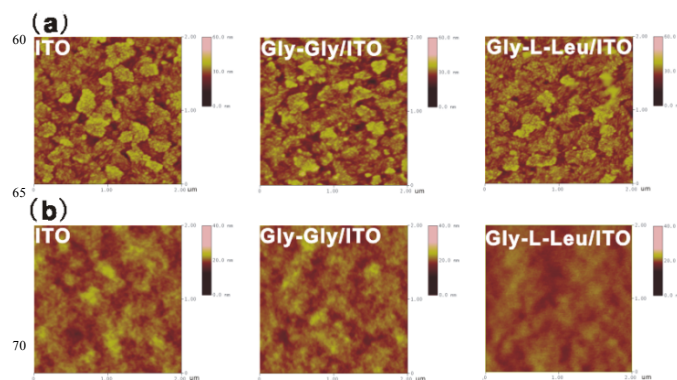


Fig. 3. (a) AFM images of bare ITO, Gly-Gly treated ITO, and Gly-L-Leu treated ITO all with a wash. (b) AFM images of PBDTTT-CF:PC₇₁BM films deposited on blank ITO and ITO modified with Gly-Gly or Gly-L-Leu.

L-Leu as shown in **Fig. 2**.

To investigate the effect of the peptides on the morphology of the ITO surface, we made AFM measurements to the ITO substrates with and without peptides SAMs. The AFM images in **Fig. 3(a)** illustrate that the roughness values of the bare ITO, the rinsed Gly-Gly treated ITO, and the rinsed Gly-L-Leu treated ITO are 3.46 nm, 3.28 nm, and 3.36 nm, respectively, indicating that the peptides SAMs modification did little to affect the morphology of the ITO surface. According to previous reports,^{24, 25} the morphology and orientation of organic layers covering the modified ITO may be affected because of the change of the surface affinity. We also compared the morphology of PBDTTT-CF:PC₇₁BM films that were spin-coated on the ITO substrate with and without Gly-Gly or Gly-L-Leu. As shown in **Fig. 3(b)**, the roughness values of the PBDTTT-CF:PC₇₁BM films on the original ITO, the Gly-Gly modified ITO, and the Gly-L-Leu modified ITO are 1.12 nm, 1.36 nm, and 1.41 nm, respectively, indicating that the modification of ITO had little effect on the morphology of the organic active layer.

Fig. 4(a) shows the UPS spectra of ITO with and without peptide modification. For all of the curves in the spectra of kinetic energy, the edge of the Fermi-level was close to the energy of the HeI source (21.22 eV), which is at near zero in the spectra of binding energy. Thus the value of work-function was determined by the cut-off edge of kinetic energy according to the method discussed in the literature.^{20, 26} The work-function of the bare ITO was 4.69 eV which was similar to the value in previous reports.²⁷ With the modification of the ITO using Gly-Gly and Gly-L-Leu, the work function was reduced to 3.33 eV and 3.63 eV, respectively. The decreased work function of the ITO was attributed to the surface dipole moment of self-assembled molecules, which is shown in **Fig. 1**. The change in the work function of substrate, $\Delta\Phi$, can be given by a simple equation:²⁸

$$\Delta\Phi(n) = eN\mu(n)\cos(\theta)/\epsilon_0\epsilon_{SAM} \quad (1)$$

where N is the surface density of the molecules, μ is the molecular dipole moment, θ is the average dipole tilt angle from the normal to the surface, and ϵ_{SAM} is the dielectric constant of the SAM. The positive amine group and the negative carboxylic group in the peptide molecule produced a large intrinsic dipole moment on the surface of the ITO. On the other hand, it was easy

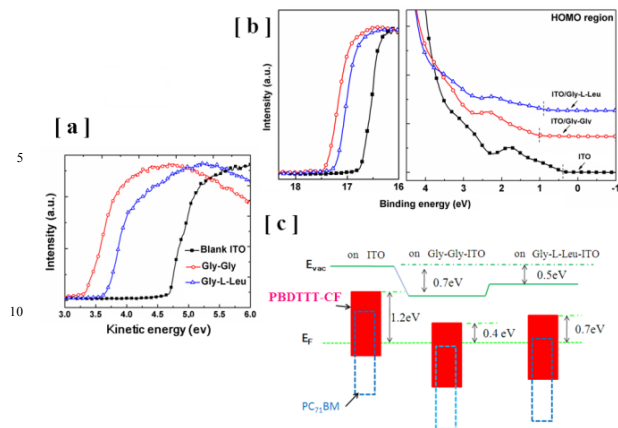


Fig. 4. (a) Normalized UPS spectra of bare ITO and ITO modified with Gly-Gly or Gly-L-Leu. (b) Normalized UPS spectra of a PBDTTT-CF:PC₇₁BM blend film spin-coated on bare ITO and ITO modified with Gly-Gly or Gly-L-Leu. (c) Schematic energy-level alignment based UPS measurements.

for the peptides to form hydrogen bonds between the carbonyl group (C=O) and the amide group (NH).^{29, 30} This is different from the other modifying molecules containing amino groups in neutral molecules or polymers and conjugated or nonconjugated polyelectrolytes.^{15, 16, 18, 23} The hydrogen bonds have stronger binding force than the Van der Waals force, which helped produce the molecule dipoles along the direction perpendicular to the ITO surface. This helps achieve a large reduction of the work-function.

To further investigate the effect of the peptides on the electronic structure of the interface between the ITO and the organic active layer. UPS measurements of an ultra-thin PBDTTT-CF:PC₇₁BM were made. **Fig. 4(b)** shows the valence band spectra of the PBDTTT-CF:PC₇₁BM on top of the bare ITO and the ITO with modification of the two peptides. The highest occupied molecular orbital (HOMO) level of the PBDTTT-CF:PC₇₁BM on the original ITO was 4.9eV, which was close to the HOMO of the PBDTTT-CF shown in the literature.³¹ This phenomenon suggests that the PBDTTT-CF was rich on top of the film surface after a vertical phase separation of PC₇₁BM to PBDTTT-CF, which was also demonstrated in another commonly used blend system of P3HT:PCBM.³²⁻³⁴ With an insertion of peptide, there was a shift of the (HOMO) toward higher BE by 0.5eV for Gly-Gly and 0.7eV for Gly-L-Leu. The energy level alignments are shown in **Fig. 4(c)**. They indicate that the modification of the ITO substrate with the Gly-Gly and the Gly-L-Leu provides, respectively, a 0.8eV and a 0.5eV decrease of the barrier height between the Fermi level and the lowest unoccupied molecular orbital (LUMO).

Fig. 5 shows the current density versus voltage (J-V) characteristics and EQE of the PBDTTT-CF:PC₇₁BM based OSCs with and without SAMs of peptides on the surface of the ITO. The device performance was optimized by altering different kinds of parameters during the process of the device fabrication (See **Fig.S1** to **Fig.S5**). As expected, the device with the bare ITO exhibited the lowest PCE, 2.12%, while the device with ITO/Gly-Gly and the device with ITO/Gly-L-Leu had PCEs of 8.13% and

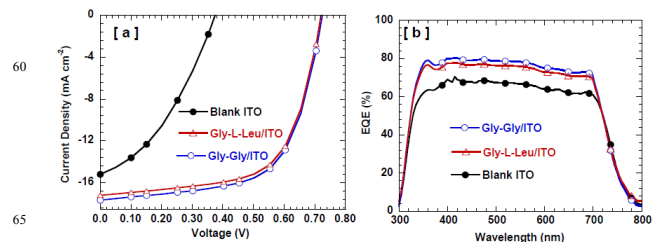


Fig. 5. J-V characteristics [a] and EQE [b] of the inverted PBDTTT-CF:PC₇₁BM based solar cells with a transparent cathode of bare ITO, Gly-Gly treated ITO, or Gly-L-Leu treated ITO.

7.92%, respectively. The simultaneously enhanced PCE was due to a comprehensive enhancement in open circuit voltage (V_{oc}), short circuit current density (J_{sc}) and filling factor (FF). The V_{oc}, the J_{sc} and the FF were increased, respectively, from 0.37 V, 15.20 mA/cm² and 38% to 0.73V, 17.69 mA/cm² and 63% for the device with Gly-Gly and to 0.72V, 17.22 mA/cm² and 64% for the device with Gly-L-Leu. The large increase in the J_{sc} and FF was attributed to the decrease of the R_s. As shown in **Fig. 5**, it was observed that the series resistance (R_s) of the devices with SAMs of peptides significantly decreased from 12.02 to 7.03 (Gly-Gly) and 6.73 (Gly-L-Leu) ohm•cm², respectively. The dramatic enhancement of the device performance can be firstly attributed to the lowered work-function of the ITO produced by the modification of peptides, which leads to a reduction of the barrier height of the electron collection interface, thus improving the ohmic contact of the ITO with the photoactive layer. The enhanced ohmic contact facilitates electron transport to the ITO, which can not only produce high efficiency electron collection to increase J_{sc} and FF, but also can help obtain the maximum achievable V_{oc}, which is dependent on the difference between the quasi-Fermi levels of the holes and the electrons.^{35, 36} The peptide modified ITO has a work function obviously lower than that of the bare ITO, which indicates that the device with peptide modified ITO has the quasi-Fermi level difference much larger than that of the device without the modification. Thus, the OSCs with the peptide modified ITO have much higher V_{oc} compared with the OSCs with the bare ITO.

The stability of the inverted OSCs was measured on condition that the devices were exposure in air without any encapsulations. **Fig. 6** shows the changes with time in V_{oc}, J_{sc}, FF and PCE of the two inverted OSCs with peptide modification and the traditional forward OSC with Ca. The forward device with Ca shows rapid degradation in the performance. After 5 hours, the efficiency of the device with Ca reduces nearly 80% from its initial value, accompanying with obvious decrease of V_{oc}, J_{sc}, and FF. However, the efficiency of the device with ITO/Peptide remains at approximately 90% after 24 hours. The results indicate that the inverted OSCs with peptide as a transparent cathode modifier exhibit a significantly improved air stability compared with the conventional device with Ca. The decreased performance of the forward device is primarily caused by the rapid reaction of metallic Ca with H₂O and O₂ from air that enters into the device through pin holes on the evaporated metal electrode. The acidic conducting polymer of PEDOT:PPSS also possibly affects the device stability because it releases acidic or ionic matters that

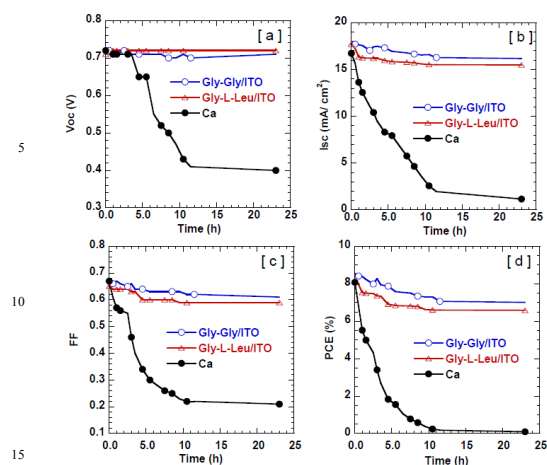


Fig.6. Changes in the PCE of the inverted OSCs with Ca, Gly-Gly/ITO, and Gly-L-Leu/ITO dependent on time.

make a damage of the ITO electrode and the active layer. In the inverted devices, there are not any active metal elements and acidic polymers. The modifying peptides are molecularly stable and chemically bonded on top of ITO, which makes the interface at the cathode of ITO more stable. Thus the OSCs with peptides modified ITO show a better air stability than the conventional device with Ca.

The performance comparison of inverted OSCs with different interlayer to modify ITO is shown in Table 1. For each modifying interlayer, we changed different deposition condition to optimize the performance. The values selected in Table 1 were the average obtained from ten devices. The devices containing solution-processed TiO_2 showed the lowest repeatability, the reason of which is the difficulty of forming TiO_2 crystals with uniform crystallinity and size by a Sol-Gel process. For the devices with a commercial polymer poly(ethylene-oxide)(PEO) as the interfacial material, although a high V_{oc} of 0.75 V and J_{sc} of 17.23 mA/cm^2 were achieved, the PCE was only 6.34% due to the low FF of 49%. The reason is that the insertion of PEO increased the series resistance due to the high insulativity of PEO. We notes that the PEO as an interfacial modifier produced significant enhanced performance of the inverted OSC based with P3HT: PCBM as an active layer according previous report.¹⁹ The different effect of PEO in P3HT and PBDTTT-CF based devices could be attributed to their different fabricating processes. For a high performance P3HT: PCBM solar cell, the active layer generally needs to undergo a slow drying process and an annealing treatment at around 110°C, which could change the formation of the PEO at the surface of ITO. PEO was also widely used as interfacial materials to achieve high performance in organic light emitting diodes (OLEDs) and OSCs with traditional forward structure.^{37,38} However, the original mechanics of the PEO in the inverted structure may be different to that of the PEO in a conventional forward structure where the reaction occurring between the -O- of PEO and the thermally evaporated metal atom can produce an n-type doping at the interface between the metal cathode and the organic layer.^{37, 39} The high electron concentration from the doping could achieve high conductivity which can make up the faults of the high insulativity of PEO for use in a forward

Table 1. Performances of the inverted PBDTTT-CF:PC₇₁BM based solar cells with TiO_2 covered ITO, PEO covered ITO, Gly-Gly treated ITO and Gly-L-Leu treated ITO.

Modifying Materials	V_{oc} (V)	J_{sc} (mA/cm^2)	Calculated J_{sc} (mA/cm^2)	FF (%)	PCE (%)	
					average	best
TiO_2	0.74	17.39	17.20	57	5.18	7.29
PEO	0.75	17.23	17.09	49	6.26	6.34
Gly-Gly	0.73	17.69	17.40	63	8.02	8.13
Gly-L-Leu	0.72	17.22	17.00	64	7.84	7.92

structure. In this work, peptide molecule is chemically adsorbed on the ITO surface so that it is insusceptible to the deposition of the organic layer on top of it. An obvious enhancement of the performance induced by the peptide modification was also observed for P3HT: PCBM based inverted solar cells (See Fig.S6). A chemisorption can also make the ITO covered with a self-assemble monolayer which effectively improves the surface properties but little changes the characteristics of bulk. On the other hand, peptides are good alternative interlayer materials because they are environmentally friendly and deposited via a healthy process. Moreover, there are many structures and types of peptides in nature, and ITO electrode is also a window electrode widely used in other optoelectronic devices such as inorganic-organic hybrid solar cells. Therefore, it is more promising to use peptides to further enhance the efficiency of organic solar cells and other optoelectronic devices.

Conclusions

In conclusion, we have demonstrated that highly efficient inverted organic solar cells can be produced by modifying the surface of indium tin oxide (ITO) cathodes with self-assembled peptide molecules. With Gly-Gly as the modifier, the inverted organic solar cells based on PBDTTT-CF:PC₇₁BM exhibited a highest PCE of 8.13% companying with a J_{sc} of 17.69 mA/cm^2 , a V_{oc} of 0.73 V and a FF of 63%. The role of peptides SAMs was to effectively decrease the work-function of the ITO surface to improve the ohmic contact between the ITO electrode and the organic active layer. As a kind of biomaterial found widely among living bodies, and with a solution processed in a water solvent, the peptides provide a low cost, healthy and environmentally friendly method for the fabrication of organic solar cells.

Experimental Section

Materials

Indium-tin-oxide (ITO) coated glass substrates with a sheet resistance of 7-10 Ω/sq were purchased from CSG Holding Co., Ltd. Peptides were purchased from Aladdin®. The electron donor material PBDTTT-CF and electron acceptor PC₇₁BM for solar cells were purchased from Solarmer Energy., Inc. and Sigma-Aldrich®, respectively, and they were used in the state in which they were received.

Modificaion of ITO

ITO substrates with patterns were first ultrasonically cleaned with detergent, deionised water, acetone, and isopropyl alcohol, for 10 min. each. The cleaned substrates were dried under a nitrogen stream and subsequently treated by UV-ozone for 15 min. After this, the substrates were soaked in a 10mM peptide aqueous solution at 90°C for 2 hours in order to form self-assembled SAMs of peptides on the surface of the ITO. Then, the substrates were rinsed with pure water to remove the residual physically adsorbed peptide molecules, and then transferred into a nitrogen glove box with a H₂O and O₂ content less than 1ppm to dry for 1 hr.

Device Fabrication

Inverted solar cells were fabricated on top of the peptide deposited ITO and the original cleaned ITO as a comparison. A solution of 10 mg ml⁻¹ PBDTTT-CF and 25 mg ml⁻¹ PC₇₁BM was blended in dichlorobenzene solvent with additive 1,8-diiodooctane (DIO)(3%v/v) and spin-coated on top of the peptides SAMs modified ITO sheets with a speed of 1000rpm for 60s. Then, they were dried in nitrogen gas at room temperature for 10 min. Finally, a 5nm thick MoO₃ layer and a 120 nm thick Al layer were successively deposited by thermal-evaporation onto the top of the active layer in a vacuum chamber with a pressure of less than 10⁻⁴ Pa. The typical active area of the devices in this study was defined at about 0.12 cm² by using a shadow mask during the anode evaporation.

Device and Film Characterization

The current densities (J)-voltage (V) characteristics of the device were recorded by a computer-controlled Keithley 2400 source meter. Simulated AM1.5 sunlight with an intensity of 100 mW/cm² was provided by a solar simulator whose light intensity was calibrated by using a Newport Oriol 91150V PV cell as a standard single-crystal Si cell. The measurement of incident photon-current conversion efficiency (IPCE) was carried out by a quantum efficiency (QE)/IPCE measurement system [SR830, Stanford Research Systems]. A standard Si photodiode calibrated from Hamamatsu was tested as a reference before each sample measurement. The standard Si photodiode was regularly calibrated by another standard Si photodiode calibrated from Newport to confirm it being degraded or not. Work-function was measured by ultraviolet photoemission spectroscopy (UPS) in ultra-high vacuum (UHV). UPS measurements were performed with an unfiltered HeI (21.22 eV) gas discharge lamp and a total instrumental energy resolution of 100meV. All the UPS measurements of the onset of photoemission for determining the work function were done using standard procedures, with a -10V bias applied to the sample to enhance the signals of with kinetic energy (KE) near zero. XPS measurements were carried out using a monochromatic Al K α source (1486.6 eV). Both the UPS and the XPS measurements were performed at room temperature. The morphology of samples was characterized by an atomic force microscopic (AFM) from Veeco NanoScope IV Multi-Mode in

tapping mode.

Notes and references

^a Research Centre for Advanced Functional Materials and Devices, Shenzhen Engineering Lab of Flexible Transparent Conductive Films, Shenzhen Key Laboratory of Advanced Materials, School of Materials Science and Engineering, Shenzhen Graduate School, Harbin Institute of Technology, Shenzhen 518055, PR China. Fax: 86-755-26033504; Tel: 86-755-26033211; E-mail: xydeng@hitsz.edu.cn

We are grateful to Mr. S. Z. Zheng, Prof. K. Y. Wong (the Chinese University of Hong Kong) and Mr. Nick K. C. Ho (the Hong Kong University of Science and Technology) for the XPS and UPS measurements. We acknowledge financial support from the Natural Scientific Research Innovation Foundation at the Harbin Institute of Technology (HIT.NSRIF, 2009142), the Shenzhen Research Foundation Project (JC201005260119A, C201105160573A, JC201104220174A) and NSFC (No. 60706017).

† Electronic Supplementary Information (ESI) available: [details of any supplementary information available should be included here]. See DOI: 10.1039/b000000x/

- B. C. Thompson, J. M. J. Frechet, *Angew. Chem. Int. Ed.* 2008, **47**, 58.
- S. Gnes, H. Neugebauer, N. S. Sariciftci, *Chem. Rev.* 2007, **107**, 1324.
- G. Yu, J. Gao, J. C. Hummelen, F. Wudl, A. J. Heeger, *Science*, 1995, **270**, 1789.
- P. Cheng, L. Ye, X.G. Zhao, J.H. Hou, Y.F. Li, X.W. Zhan. *Energy Environ. Sci.* DOI: 10.1039/c3ee43041c.
- G. Li, C.-W. Chu, V. Shrotriya, J. Huang, Y. Yang, *Appl. Phys. Lett.* 2006, **88**, 253503.
- S. White, D. C. Olson, S. E. Shaheen, N. Kopidakis, D. S. Ginley, *Appl. Phys. Lett.* 2006, **89**, 143517.
- S. K. Hau, H.-L. Yip, N. S. Baek, J. Zou, K. O'Malley, A. K.-Y. Jen, *Appl. Phys. Lett.* 2008, **92**, 253301.
- Y. M. Sun, J. H. Seo, C. J. Takacs, J. Seifert, A. J. Heeger. *Adv. Mater.* 2011, **23**, 1679.
- Z. Xu, L. M. Chen, G. Yang, C. H. Huang, J. Hou, Y. Wu, G. Li, C. S. Hsu, Y. Yang, *Adv. Funct. Mater.* 2009, **19**, 1227.
- M. Lira-Cantu, A. Chafiq, J. Faissat, I. Gonzalez-Valls, Y.H. Yu, *Sol. Ener. Mater&Sol. Cells*, 2011, **95**, 1362.
- S. Bai, Z.W. Wu, X.L. Xu, Y.Z. Jin, B.Q. Sun, X.J. Guo, S.S. He, X. Wang, Z.Z. Ye, H.X. Wei, X.Y. Han, W.L. Ma, *Appl. Phys. Lett.* 2012, **100**, 203906.
- S. Chen, C. E. Small, C. M. Amb, J. Subbiah, T.-H. Lai, S.-W. Tsang, J. R. Manders, J.R. Reynolds, F. So, *Adv. Ener. Mater.* 2012, **2**, 1333.
- G. Li, C.-W. Chu, V. Shrotriya, J. Huang, Y. Yang, *Appl. Phys. Lett.* 2006, **88**, 253503.
- K. Zilberberg, A. Behrendt, M. Kraft, U. Scherf, T. Riedl, *Org. Electronics*, 2013, **14**, 951.
- H. Kang, S. Hong, J. Lee, K. Lee, *Adv. Mater.* 2012, **24**, 3005.
- Z.C. He, C.M. Zhong, S.J. Su, M. Xu, H.B. Wu, Y. Cao, *Nature Photon.* 2012, **6**, 951.
- J. W. Shim, H. Cheun, J. Meyer, C. Fuentes-Hernandez, A. Dindar, Y. H. Zhou, D. K. Hwang, A. Kahn and B. Kippelen, *Appl. Phys. Lett.* 2012, **101**, 073303.
- Y. Zhou, C. Fuentes-Hernandez, J. Shim, J. Meyer, A. J. Giordano, H. Li, P. Winget, T. Papadopoulos, H. Cheun, J. Kim, M. Fenoll, A. Dindar, W. Haske, E. Najafabadi, T. M. Khan, H. Sojoudi, S. Barlow, S. Graham, J.-L. Brédas, S. R. Marder, A. Kahn, B. Kippelen, *Science*, 2012, **336**, 327.
- Y. Zhou, F. Li, S. Barrau, W. Tian, O. Inganäs, and F. Zhang, *Sol. Energy Mater. Sol. Cells* 2009, **93**, 497.
- K. Sun, B. Zhao, A. Kumar, K. Zeng, J. Ouyang, *ACS Appl. Mater. Interfaces.* 2012, **4**, 2009.
- F. Nüesch, L. J. Rothberg, E. W. Forsythe, Q. T. Le, Y. Gao, *Appl. Phys. Lett.* 1999, **74**, 880.

- 22 W. Osikowicz, X. Crispin, C. Tengstedt, L. Lindell, T. Kugler, and W. R. Salaneck, *Appl. Phys. Lett.* 2004, **85**, 1616.
- 23 M. Song, J.-W. Kang, D.H. Kim, J.D. Kwon, S.G. Park, S. Nam, S. Jo, S.Y. Ryu, C.S. Kim, *Appl. Phys. Lett.* 2013, **102**, 143303.
- 5 24 J. Cui, Q. L. Huang, J. G. C. Veinot, H. Yan, T. J. Marks, *Adv. Mater.* 2002, **14**, 565.
- 25 C. C. Hsiao, C. H. Chang, M. C. Hung, N. J. Yang, S. A. Chen, *Appl. Phys. Lett.* 2005, **86**, 223505.
- 26 J.-H. Lee, J.-J. Kim, *Phys. Status Solidi A* . 2012, **209**, 1399.
- 10 27 I. D. Parker, *J. Appl. Phys.* 1994, **75**, 1656.
- 28 S. Lacher, Y. Matsuo, E. Nakamura, *J. Am. Chem. Soc.* 2011, **133**, 16997.
- 29 S. Aravinda, S. Datta, N. Shamala, P. Balaram, *Angew. Chem. Int. Ed.* 2004, **43**, 6728.
- 15 30 H. G. Carl, *Acta Cryst.* 1989, **B45**, 390.
- 31 H.-Y. Chen, J. H. Hou, S.Q. Zhang, Y.Y. Liang, G.W. Yang, Y. Yang, L.P. Yu, Y. Wu, G. Li, *Nature Photon.* 2009, **3**, 650.
- 32 W.-H. Tseng, M.-H. Chen, J.-Y. Wang, C.-T. Tseng, H. Lo, P.-S. Wang, C.-I. Wu, *Sol. Energy Mater. Sol. Cells*, 2011, **95**, 3424.
- 20 33 D. Gao, M. G. Helander, Z. B. Wang, D. P. Puzzo, M. T. Greiner, Z. H. Lu, *Adv. Mater.* 2010, **22**, 5404.
- 34 L. Jiang, A.Y. Li, X.Y. Deng, S.Z. Zheng, K.-Y. Wong, *Appl. Phys. Lett.* 2013, **102**, 013303 .
- 35 E.L. Ratcliff, B. Zacher, N.R. Armstrong, *J. Phys. Chem. Lett.*, 2011, **2**, 1337.
- 25 36 V. D. Mihailetschi, P. W. M. Blom, J. C. Hummelen, M. T. Rispens, *J. Appl. Phys.*, 2003, **94**, 6849.
- 37 J.-Y. Jeng, M.-W. Lin, Y.-J. Hsu, T.-C. Wen , T.-F. Guo, *Adv. Energy Mater.* 2011, **1**, 1192.
- 30 38 T.-F. Guo, F.-S. Yang, Z.-J. Tsai, T.-C. Wen, S.-N. Hsieh, Y.-S. Fu, *Appl. Phys. Lett.* 2005, **87**, 013504 .
- 39 X. Y. Deng, W. M. Lau, K. Y. Wong, K. H. Low, H. F. Chow, Y. Cao, *Appl. Phys. Lett.* 2004, **84**, 3522.